

Effect of oxygen on emulsion polymerisation kinetics: a study by reaction calorimetry

Lourdes López de Arbina, Luis M. Gugliotta†, María J. Barandiaran and José M. Asua*

Grupo de Ingeniería Química, Departamento de Química Aplicada, Facultad de Ciencias Químicas, Universidad del País Vasco/Euskal Herriko Unibertsitatea, Apdo. 1072, 20080 San Sebastián, Spain

(Accepted 12 November 1997)

The influence of oxygen on the kinetics of chemically initiated seeded emulsion homopolymerisation of styrene and the seeded emulsion copolymerisation of styrene/butyl acrylate was investigated by reaction calorimetry. A decrease of the inhibition period and an increase of the polymerisation rate have been observed when the system is purged with nitrogen. It has also been seen that oxygen has a great influence on the polymerisation kinetics, producing not only inhibition, but also decreasing the reaction rate. An increase of the dependence of the average number of radicals per particle with the initiator concentration with respect to theoretical predictions was observed in the presence of oxygen. The overall experimental results show that, after an inhibition period, there is a continuous flow of oxygen from the gas phase, which causes the retardation of the polymerisation rate. © 1998 Elsevier Science Ltd. All rights reserved.

(Keywords: emulsion polymerisation; oxygen; inhibition)

INTRODUCTION

Emulsion polymerisation is a free radical polymerisation whose kinetics is severely affected by the presence of small amounts of inhibitors and retarders. These substances are polymerisation suppressors of different degrees of effectiveness¹. Inhibitors completely stop the polymerisation, whereas retarders are less efficient and cause only a reduction of the polymerisation rate. Inhibition and retardation are often the cause of run-to-run irreproducibility.

Oxygen is a common and powerful polymerisation suppressor that is often considered to be an ideal inhibitor, i.e. it has to disappear completely from the reaction mixture to start the polymerisation^{2–8}. However, data that questioned the ideal behavior of oxygen as an inhibitor have been reported^{9–15}. Thus, Hasan⁹ found that below a critical concentration oxygen accelerated the thermal emulsion polymerisation of styrene carried out in the absence of chemical initiator and using sodium lauryl sulphate as emulsifier. Above the critical concentration oxygen inhibited the polymerisation. Schoonbrood¹⁰ studied the kinetics of the seeded emulsion polymerisation of styrene and methyl acrylate by means of consecutive γ -relaxation experiments finding that, after the first insertion in the γ -radiation source, the polymerisation rate was slower than in the consecutive runs in which the polymerisation rate was always the same. This was taken as evidence that species present in the reaction, presumably oxygen, acted as a retarder of the reaction rate. However, Adams¹¹ demonstrated that the difference between the first and subsequent

polymerisation rates can be accounted for by the difference between the initial zero polymerisation rate at the beginning of the first insertion and the non-zero polymerisation rates at the beginning of all subsequent insertions. Recently, Vega *et al.*¹² noted that the presence of variable amounts of O₂ distorted the conversion profile in the emulsion copolymerisation of acrylonitrile and butadiene carried out in an industrial reactor. Hattori *et al.*¹³ found that the presence of oxygen affects the colloidal stability during the dispersion polymerisation of divinylbenzene in methanol. They proposed that the oxygen promotes the grafting of poly(divinylbenzene) to the poly(vinylpyrrolidone) stabiliser molecules because the particle size decreased when the concentration of oxygen increased. Similar results were reported by Burnett *et al.*¹⁴, whereas the opposite trend has been reported by Kourti¹⁵ and Sáenz and Asua¹⁶. However, the last authors¹⁶ did not interpret their results in terms of non-ideal behavior of the oxygen as an inhibitor, but as a retardation caused by the slow diffusion of the oxygen from the head space to the reaction mixture. This mechanism was proved by Nomura *et al.*¹⁷, Kiparissides *et al.*¹⁸ and Donescu *et al.*¹⁹, who found that, in the presence of oxygen, the polymerisation rate decreased when the agitation rate increased, namely when the oxygen mass transport rate from the head space to the aqueous phase increased.

Kinetic studies in emulsion polymerisation are normally performed in absence of oxygen. However, in reactions carried out in industry or even in the laboratory it is difficult to completely eliminate this impurity. For this reason, it is important to have some additional insight into its influence on polymerisation rates.

In this paper the effect of the oxygen on the kinetics of the seeded emulsion homopolymerisation of styrene, and the seeded emulsion copolymerisation of styrene/butyl acrylate, was investigated by reaction calorimetry.

* To whom correspondence should be addressed

† On leave from INTEC (Consejo Nacional de Investigaciones Científicas y Técnicas and Universidad Nacional del Litoral, Santa Fe, República Argentina).

Table 1 Recipes used for the preparation of the polystyrene seeds ($T = 90^{\circ}\text{C}$)

Seed	Styrene (g)	MA-80 (g)	H ₂ O (g)	NaHCO ₃ (g)	K ₂ S ₂ O ₈ (g)	d_n (nm)
S1	403	20.47	959	1.5	1.5	79
S2	97	18.40	1026	1	1	84
S3	473	19.82	1125	1.8	1.8	108

Table 2 Recipes used for the preparation of the polystyrene/polybutyl acrylate seeds

Seed	Step	St (g)	BuA (g)	SLS (g)	H ₂ O (g)	NaH ₂ PO ₄ (g)	K ₂ S ₂ O ₈ (g)	T ($^{\circ}\text{C}$)	Feed time (h)	d_n (nm)
AS1	1	273.6	182.4	40.2	1520	4.2	4.2	70	—	—
	2	477.5	318.5	—	2600	—	5	75	9	63
Seed		St (g)	BuA (g)	SLS (g)	H ₂ O (g)	Seed AS1 (g)	Na ₂ S ₂ O ₈ (g)	T ($^{\circ}\text{C}$)		
AS2		67.3	44.9	1.1	1156.2	39.0	0.5	60		100

Table 3 Recipes used in the first series of styrene emulsion homopolymerizations (without N₂ purge)

Run	$N_p \times 10^{-13}$ (particles per cm ³ of water)	$[\text{Na}_2\text{S}_2\text{O}_8] \times 10^7$ (mol cm ⁻³ of water)
Seed S3		
Head space = 150 cm ³ , liquid phase = 100 cm ³		
1H1	4.7	40
1H2	4.7	10
1H3	9.4	80
1H4	9.4	40
1H5	9.4	10
1H6	15.6	80
1H7	15.6	40
1H8	15.6	10
Head space = 70 cm ³ , liquid phase = 180 cm ³		
1H9	4.7	
Seed S2		
Head space = 150 cm ³ , liquid phase = 100 cm ³		
1H10	10.4	80
1H11	10.4	40
1H12	10.4	20
1H13	10.4	10
1H14	19.1	80
1H15	19.1	40
1H16	19.1	20
1H17	19.1	10
1H18	42.7	80
1H19	42.7	20
1H20	42.7	10

Table 4 Recipes used in the second series of styrene emulsion homopolymerizations (swelling and calibration under N₂ blanket, but reactions without N₂ purge)

Run	$N_p \times 10^{-13}$ (particles per cm ³ of water)	$[\text{Na}_2\text{S}_2\text{O}_8] \times 10^7$ (mol cm ⁻³ of water)
Seed S3 (head space = 150 cm ³ , liquid phase = 100 cm ³)		
2H1	4.7	5
2H2	4.7	2.5
2H3	9.4	40
2H4	9.4	20
2H5	9.4	10
2H6	9.4	5
2H7	9.4	2.5

EXPERIMENTAL

Styrene (St) was purified by distillation under reduced pressure and stored at -18°C until used. Butyl acrylate (BuA) was washed several times first with a 10% weight aqueous solution of sodium hydroxide and afterwards with distilled-and-deionised water (DDI) until wash waters were neutral. Then, it was dried over CaCl₂ and distilled under reduced pressure and stored at -18°C until used. K₂S₂O₈

(Merck), Na₂S₂O₈ (Merck), NaHCO₃ (Merck), NaH₂PO₄ (Merck), Aerosol MA-80 (sodium dihexyl sulfosuccinate, Cyanamid) and sodium lauryl sulphate (SLS, Henkel) were used as received.

To study the effect of the oxygen on the homopolymerisation of styrene, three monodisperse seed latexes (S1, S2 and S3) were prepared at 90°C in a batch reactor using the recipes presented in *Table 1*. Before being used in the kinetic runs, the seeds, whose number average diameters (d_n) (measured by transmission electron microscopy (TEM)) are also included in *Table 1*, were cleaned by dialysis. To carry out the seeded emulsion copolymerisations, two monodisperse seeds were prepared (AS1 and AS2). The smaller seed (AS1) was prepared in two steps, following the recipe given in *Table 2*. The first step was carried out in a batch reactor at 70°C , and the second in a semibatch reactor under starved conditions, at 75°C . The latex obtained in the first step was used as seed in the second one. The larger seed (AS2) was prepared by swelling the latex AS1 with a mixture of both monomers, which were subsequently polymerised in batch at 60°C . Before the use in the kinetic runs, both AS1 and AS2 latexes were kept at 80°C during 48 h, in order to completely destroy the initiator. *Table 2* presents the average number diameter of these seed latexes as measured by TEM.

The styrene emulsion homopolymerisations were conducted in a calorimeter reactor (Chemisens-Thermometric RM-1). The total volume of the reactor vessel is 250 cm³, although the volume of the reaction mixture in the kinetic runs ranged between 100 and 150 cm³. The reaction mixture was agitated at 300 r.p.m. by a propeller stirrer. The seeded emulsion copolymerisations of styrene/butyl acrylate were carried out in the calorimeter reactor RC-1 (Mettler), equipped with an AP01 glass reactor. The total volume of this reactor is 2.3 l, although the volume of the reaction mixture in the kinetic runs was 1.3 l. The reaction mixture was agitated at 150 r.p.m. by an anchor stirrer.

For the kinetic investigation, all the seeded polymerisations were conducted in batch at 60°C , starting the reactions under interval II conditions (monomer droplets present in the reactor), with a 3/1 monomer/seed weight ratio. Prior to the polymerisation, the seed and all of the components of the recipe with the exception of the initiator and the water needed to prepare the initiator solution were mixed and kept under agitation at room temperature for 16 h. This time was enough to reach the equilibrium swelling. The reactor was heated to the polymerisation temperature (60°C). Then, the reaction mixture was charged into the reactor and the calorimetric reactor calibrated. The polymerisation was started by injecting the initiator solution.

Table 5 Recipes used in the third series of styrene emulsion homopolymerizations (swelling, calibration and reactions under N₂ purge)

	Run			
	3H1	3H2	3H3	3H4
Seed S1 ^a				
Nitrogen flow × 10 ² (cm ³ s ⁻¹)	0.7	1.4	3.0	5.8
Number of τ until the beginning of the polymerization ^b	3.6	6.9	15.8	30.6

^aN_p = 14.4 × 10¹³ particles cm⁻³ of water; [Na₂S₂O₈] = 2.5 × 10⁻⁷ mol cm⁻³ of water; head space = 130 cm³; liquid phase = 120 cm³
^bτ = Residence time based on the head space volume

Table 6 Recipes used in the first series of styrene/butyl acrylate emulsion copolymerizations (without N₂ purge)

Run	N _p × 10 ⁻¹³ (particles per cm ³ of water)	[Na ₂ S ₂ O ₈] × 10 ⁷ (mol cm ⁻³ of water)
Seed AS1 ^a		
1C1	24.0	160
1C2	24.0	120
1C3	24.0	40
1C4	24.0	30
1C5	24.0	20
1C6	24.0	15
1C7	24.0	10
1C8	47.9	160
1C9	47.9	120
1C10	47.9	80
1C11	47.9	40
1C12	47.9	20
1C13	47.9	15
1C14	47.9	10

Table 7 Recipes used in the second series of styrene/butyl acrylate emulsion copolymerizations (slow N₂ flow along the reaction)

Run	N _p × 10 ⁻¹³ (particles per cm ³ of water)	[Na ₂ S ₂ O ₈] × 10 ⁷ (mol cm ⁻³ of water)
Seed AS2 ^a		
2C1	10.7	40
2C2	10.7	20
2C3	10.7	10
2C4	10.7	5
2C5	10.7	2.5
2C6	10.7	0.625

^aHead space = 1000 cm³, liquid phase = 1300 cm³

Three series of experiments were carried out to study the influence of the oxygen on the homopolymerisation of styrene. The first was carried out using the recipes given in *Table 3* and no nitrogen purge. Two seeds of different size (S2 of $d_n = 84$ nm and S3 of $d_n = 108$ nm) were used and the concentration of initiator, the concentration of polymer particles (N_p), and head space/liquid phase volume ratio were varied. The second series was carried out with the recipes presented in *Table 4*. In this series, the swelling mixture was purged with nitrogen (purity, 99.995%) for 1 h (flow rate, 0.1 cm³ s⁻¹) and the heating of the reactor, calibration and stabilisation were carried out under a nitrogen blanket. However, the flow of nitrogen was stopped when the initiator solution was injected. Both initiator concentration and concentration of polymer particles were varied in this series. *Table 5* presents the recipes used in the third series of experiments. In this series, the swelling mixture was purged with nitrogen (purity, 99.995%) for 1 h

(flow rate, 0.2 cm³ s⁻¹) and a stream of nitrogen was introduced into the reactor during the heating, calibration, stabilisation and reaction. Runs using different nitrogen flow rates were carried out.

Two series of experiments were carried out to study the influence of the oxygen on the copolymerisation of styrene/butyl acrylate. The first series was similar to the first series of the study of the homopolymerisation of styrene (namely in the absence of N₂ purge), where the initiator concentration and the concentration of polymer particles were varied, according to recipes given in *Table 6*. In the second series of experiments, a slow (not measured) nitrogen flow was used only after introducing all the reactants in the reactor. In this copolymerisation group, only the initiator concentration was varied. The recipes are given in *Table 7*.

All the polymerisations were examined by TEM to check for new nucleations.

The calorimetric conversion X_{TC} was calculated from the measured polymerisation heat flow as:

$$X_{TC}(t) = \frac{\int_0^t Q_r(t) dt}{\int_0^{t_{ff}} Q_r(t) dt} X_{TC,ff}$$

where Q_r is the heat generation rate of the reaction and $X_{TC,ff}$ is the final calorimetric conversion. In the case of the homopolymerisation, the calorimetric and gravimetric conversions are coincident. Hence, $X_{TC,ff}$ can be calculated from gravimetric measurements. In the case of the copolymerisation, however, both conversions are different. The difference increases as the homopolymerisation heats ($-\Delta H_i$), the reactivities of the monomers and the molecular weights of the monomers are more different. The calorimetric conversion at the end of the process, assuming that the cross-propagation heat is equal to the homopolymerisation heat, is calculated as follows:

$$X_{TC,ff} = \frac{\sum M_{i0} X_{i,ff} (-\Delta H_i)}{\sum M_{i0} (-\Delta H_i)}$$

where $X_{i,ff}$ is the molar conversion of monomer i at the end of the process determined by combining gravimetry and gas chromatography and M_{i0} is the amount of monomer i initially charged into the reactor.

RESULTS AND DISCUSSION

Styrene emulsion homopolymerisation

Figures 1–6 present the effect of the initiator concentration on the conversion profiles in the first series of experiments (Runs 1H1–1H20, except 1H9), carried out without elimination of oxygen. Long inhibition periods were observed in some of the polymerisations. The inhibition periods are reported in *Table 8*. It can be seen that the inhibition period decreased as the initiator concentration increased and no inhibition was observed for the runs carried out with high initiator concentrations. In addition, the inhibition period increased with the particle concentration for the polymerisations carried out with low initiator concentrations. This last effect may be due to the fact that the solubility of the oxygen in the organic phase (7×10^{-6} mol cm⁻³, 760 mm, 50°C²⁰) is higher than the solubility in the aqueous phase (1.5×10^{-7} mol cm⁻³, 760 mm, 60°C²¹); hence, an increase of the particle concentration, which are swollen by monomer, increases

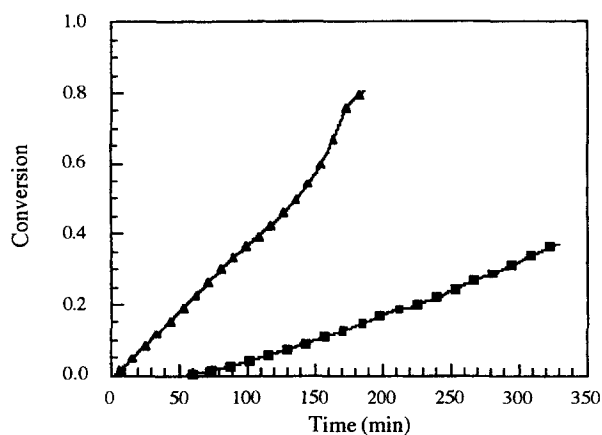


Figure 1 Evolution of the conversion in the first series of runs of styrene emulsion homopolymerisation. (\blacktriangle) 1H1, $[I_2] = 40 \times 10^{-7} \text{ mol cm}^{-3}$ of water; (\blacksquare) 1H2, $[I_2] = 10 \times 10^{-7} \text{ mol cm}^{-3}$ of water (seed S3, $N_p = 4.7 \times 10^{13}$ particles per cm^3 of water)

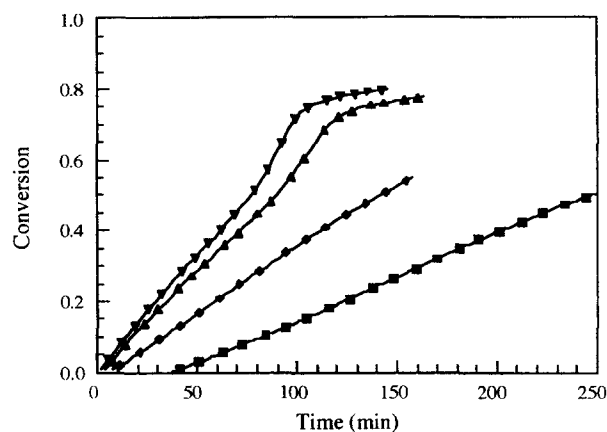


Figure 4 Evolution of the conversion in the first series of runs of styrene emulsion homopolymerisation. (\blacktriangledown) 1H10, $[I_2] = 80 \times 10^{-7} \text{ mol cm}^{-3}$ of water; (\blacktriangle) 1H11, $[I_2] = 40 \times 10^{-7} \text{ mol cm}^{-3}$ of water; (\blacklozenge) 1H12, $[I_2] = 20 \times 10^{-7} \text{ mol cm}^{-3}$ of water; (\blacksquare) 1H13, $[I_2] = 10 \times 10^{-7} \text{ mol cm}^{-3}$ of water (seed S2, $N_p = 10.4 \times 10^{13}$ particles per cm^3 of water)

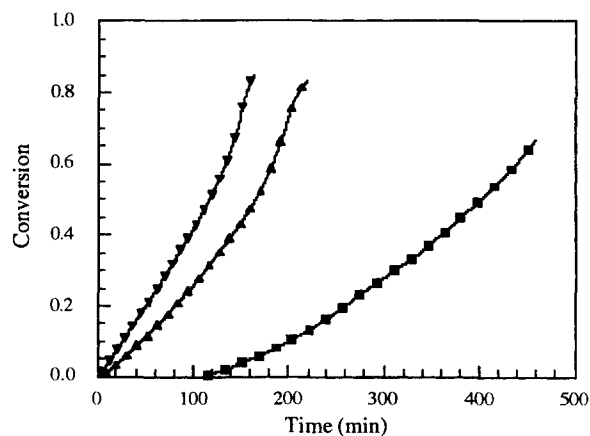


Figure 2 Evolution of the conversion in the first series of runs of styrene emulsion homopolymerisation. (\blacktriangledown) 1H3, $[I_2] = 80 \times 10^{-7} \text{ mol cm}^{-3}$ of water; (\blacktriangle) 1H4, $[I_2] = 40 \times 10^{-7} \text{ mol cm}^{-3}$ of water; (\blacksquare) 1H5, $[I_2] = 10 \times 10^{-7} \text{ mol cm}^{-3}$ of water (seed S3, $N_p = 9.4 \times 10^{13}$ particles per cm^3 of water)

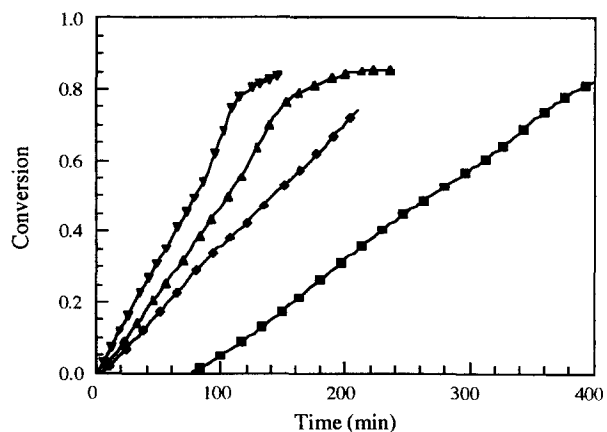


Figure 5 Evolution of the conversion in the first series of runs of styrene emulsion homopolymerisation. (\blacktriangledown) 1H14, $[I_2] = 80 \times 10^{-7} \text{ mol cm}^{-3}$ of water; (\blacktriangle) 1H15, $[I_2] = 40 \times 10^{-7} \text{ mol cm}^{-3}$ of water; (\blacklozenge) 1H16, $[I_2] = 20 \times 10^{-7} \text{ mol cm}^{-3}$ of water; (\blacksquare) 1H17, $[I_2] = 10 \times 10^{-7} \text{ mol cm}^{-3}$ of water (seed S2, $N_p = 19.1 \times 10^{13}$ particles per cm^3 of water)

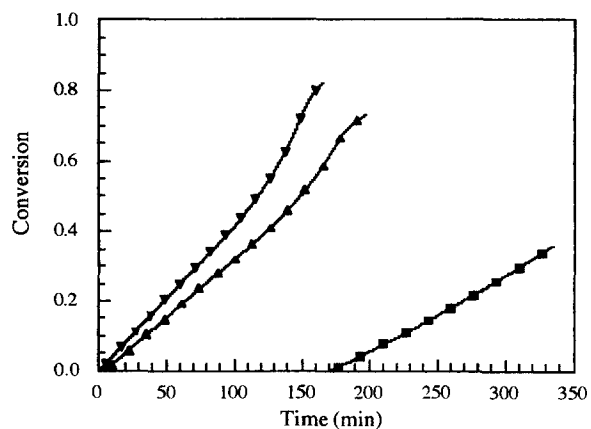


Figure 3 Evolution of the conversion in the first series of runs of styrene emulsion homopolymerisation. (\blacktriangledown) 1H6, $[I_2] = 80 \times 10^{-7} \text{ mol cm}^{-3}$ of water; (\blacktriangle) 1H7, $[I_2] = 40 \times 10^{-7} \text{ mol cm}^{-3}$ of water; (\blacksquare) 1H8, $[I_2] = 10 \times 10^{-7} \text{ mol cm}^{-3}$ of water (seed S3, $N_p = 15.6 \times 10^{13}$ particles per cm^3 of water)

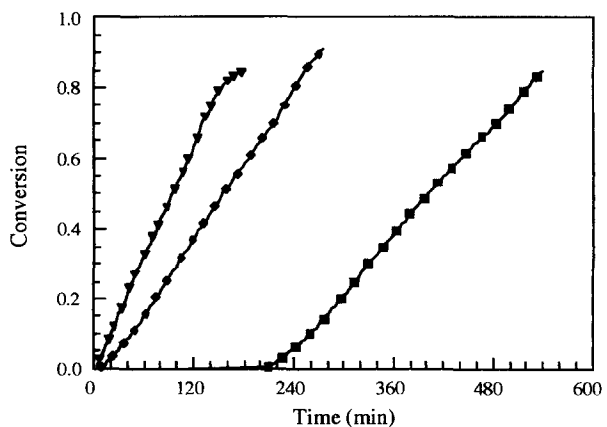


Figure 6 Evolution of the conversion in the first series of runs of styrene emulsion homopolymerisation. (\blacktriangledown) 1H18, $[I_2] = 80 \times 10^{-7} \text{ mol cm}^{-3}$ of water; (\blacklozenge) 1H19, $[I_2] = 20 \times 10^{-7} \text{ mol cm}^{-3}$ of water; (\blacksquare) 1H20, $[I_2] = 10 \times 10^{-7} \text{ mol cm}^{-3}$ of water (seed S2, $N_p = 42.7 \times 10^{13}$ particles per cm^3 of water)

Table 8 Inhibition periods observed in the different homopolymerizations

Run	$N_p \times 10^{-13}$ (particles cm^{-3} of water)	$[\text{Na}_2\text{S}_2\text{O}_8] \times 10^7$ (mol cm^{-3} of water)	Nitrogen flow ($\text{cm}^3 \text{s}^{-1}$)	Inhibition period (min)
1H1	4.7	40	No	2
1H2	4.7	10	No	53
1H3	9.4	80	No	0
1H4	9.4	40	No	3
1H5	9.4	10	No	107
1H6	15.6	80	No	0
1H7	15.6	40	No	3
1H8	15.6	10	No	169
1H9	4.7	10	No	0
1H10	10.4	80	No	0
1H11	10.4	40	No	1
1H12	10.4	20	No	4
1H13	10.4	10	No	35
1H14	19.1	80	No	0
1H15	19.1	40	No	2
1H16	19.1	20	No	2
1H17	19.1	10	No	73
1H18	42.7	80	No	0
1H19	42.7	20	No	4
1H20	42.7	10	No	203
2H1	4.7	5	Yes	0
2H2	4.7	2.5	Yes	6
2H3	9.4	40	Yes	0
2H4	9.4	20	Yes	0
2H5	9.4	10	Yes	0
2H6	9.4	5	Yes	0
2H7	9.4	2.5	Yes	2
3H1	14.4	2.5	0.7×10^{-2}	243
3H2	14.4	2.5	1.4×10^{-2}	146
3H3	14.4	2.5	3.0×10^{-2}	2
3H4	14.4	2.5	5.8×10^{-2}	0

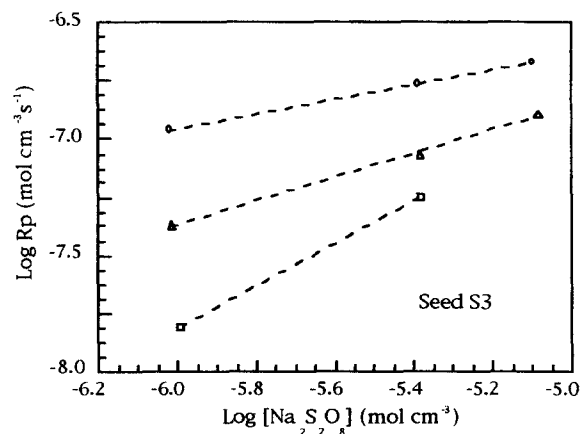
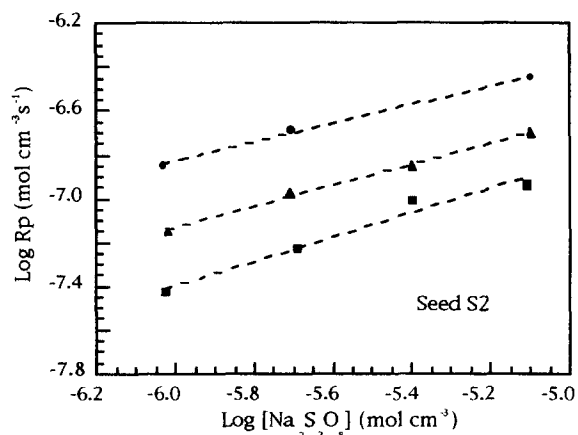

Figure 7 Effect of the initiator concentration on the polymerisation rate measured at $x = 0.1$ for the runs of the first series of styrene emulsion homopolymerizations carried out using a head space/liquid-phase volume ratio of 1.5, $N_p \times 10^{-13}$ particles per cm^3 of water: (■) 10.4; (▲) 19.1; (●) 42.7; (□) 4.7; (△) 9.4; (○) 15.6

Table 9 Values of the \bar{n} ranges and slopes of the runs plotted in Figures 1–6

Seed	$N_p \times 10^{-13}$ (particles per cm^3 of water)	Slope	\bar{n} range
S2	10.4	0.56	0.12–0.38
S2	19.1	0.49	0.13–0.37
S2	42.7	0.44	0.12–0.30
S3	4.7	0.94	0.11–0.43
S3	9.4	0.52	0.15–0.47
S3	15.6	0.31	0.25–0.48

the total oxygen in the medium, and subsequently the inhibition period. Furthermore, it has to be pointed out that, as in these runs both the total volume of the reaction and the initial monomer/polymer ratio were held constant, an increase of the volume of the organic phase due to an increase of the particle concentration, and therefore of the amount of monomer, is balanced with a decrease of the aqueous phase, and hence in the total amount of initiator.

Figure 7 presents the effect of the initiator concentration on the polymerisation rate, R_p , measured at 10% conversion for the experiments of the first series carried out with a head space/liquid phase volume ratio of 1.5. It can be seen that the effect of the initiator concentration is more pronounced for the runs carried out with small polymer particle concentrations. Table 9 presents the values of the slopes of the straight lines in Figure 7, together with the range average number of radicals per particle (\bar{n}) calculated by taking into account the number of particles, the value of the propagation reaction rate, $k_p = 3.4 \times 10^5 \text{ cm}^3 \text{ mol}^{-1} \text{ s}^{-1}$ ²² and the monomer concentration in the polymer particles, $[\text{M}]_p = 5.01 \times 10^{-3} \text{ mol cm}^{-3}$ ²³. The expected dependence of the polymerisation rate on the initiator concentration ranges from a zero-order for Smith-Ewart case 2 ($\bar{n} = 0.5$)

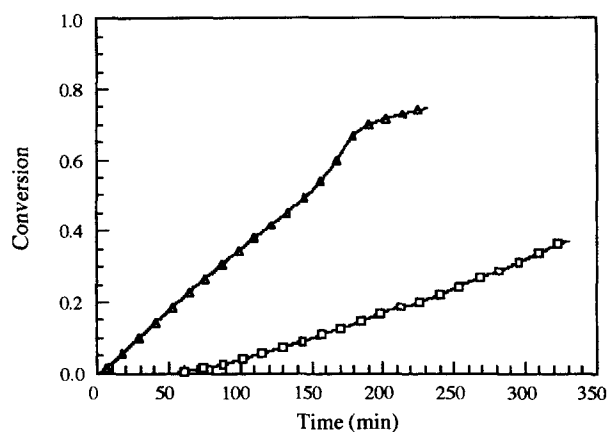


Figure 8 Effect of the head space/liquid-phase volume ratio on the time evolution of the conversion. Legend: (\square) run 1H2, head space/liquid-phase = 1.5; (Δ) run 1H9, head space/liquid-phase = 0.39 ($N_p = 4.7 \times 10^{13}$ particles per cm^3 of water; $[I_2] = 10 \times 10^{-7}$ mol cm^{-3} of water)

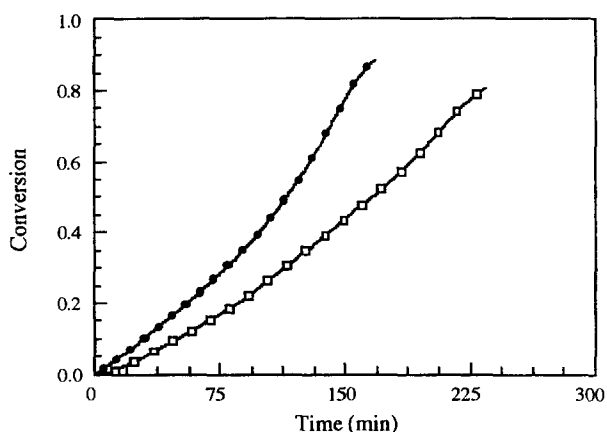


Figure 9 Evolution of the conversion in the second series of styrene emulsion homopolymerisation. (\bullet) 2H1, $[I_2] = 5 \times 10^{-7}$ mol cm^{-3} of water; (\square) 2H2, $[I_2] = 2.5 \times 10^{-7}$ mol cm^{-3} of water (see S3, $N_p = 4.7 \times 10^{13}$ particles per cm^3 of water)

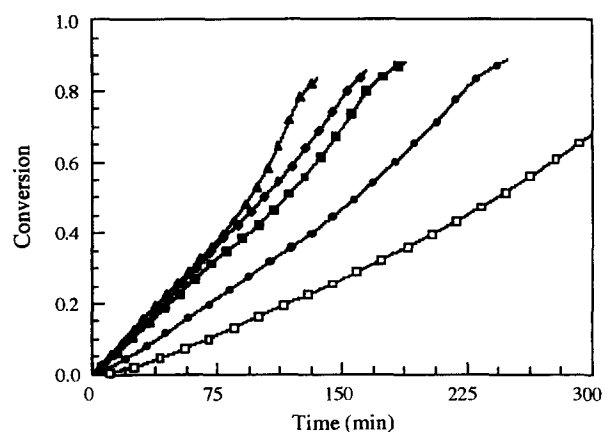


Figure 10 Evolution of the conversion in the second series of styrene emulsion homopolymerisation. (\blacktriangle) 2H3, $[I_2] = 40 \times 10^{-7}$ mol cm^{-3} of water; (\blacklozenge) 2H4, $[I_2] = 20 \times 10^{-7}$ mol cm^{-3} of water; (\blacksquare) 2H5, $[I_2] = 10 \times 10^{-7}$ mol cm^{-3} of water; (\bullet) 2H6, $[I_2] = 5 \times 10^{-7}$ mol cm^{-3} of water; (\square) 2H7, $[I_2] = 2.5 \times 10^{-7}$ mol cm^{-3} of water (see S3, $N_p = 9.4 \times 10^{13}$ particles per cm^3 of water)

kinetics to a 0.5-order for Smith-Ewart cases 1 ($\bar{n} < 0.15$) and 3 ($\bar{n} > 1$)²⁴. Comparison of these values with those presented in Table 9 shows that the observed dependence

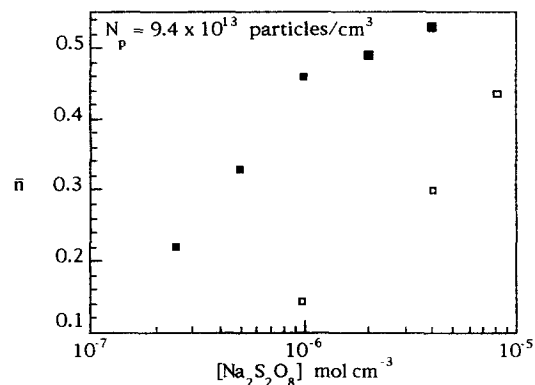
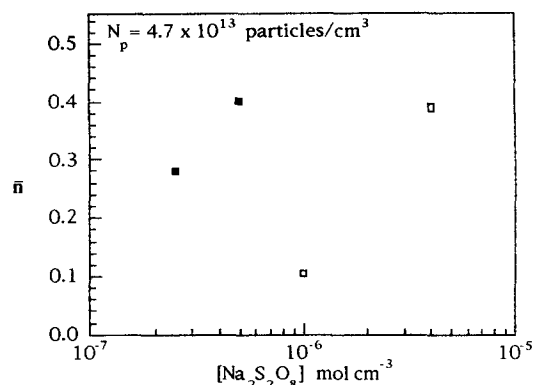


Figure 11 Effect of the nitrogen purge on \bar{n} . Legend: (\square) first series of experiments; (\blacksquare) second series

was substantially higher than that predicted by the theory. Which means that the oxygen not only inhibits but affects the polymerisation rate. Even after the end of the inhibition period, when the polymerisation starts, there is still oxygen in the reaction mixture. This oxygen present can come from the one dissolved in the head space, which slowly diffuses into the water and organic phases. In order to check the importance of this process, the effect of the head space/liquid-phase volume ratio on the polymerisation rate must be investigated.

Figure 8 presents the effect of the gas-phase/liquid-phase volume ratio on the time evolution of the conversion. It can be seen that the polymerisation rate increased and the inhibition decreased when the head space/liquid-phase volume ratio decreased. This is an indication that the gas phase plays an important role in the retardation of the polymerisation. Kolthoff and Dale⁷ and Mørk²⁵ also found that the inhibition period decreased when the head space/liquid-phase volume fraction decreased, although they did not observe any effect on the polymerisation rate.

A possible explanation for these results is as follows: at the beginning of the process, the aqueous phase is saturated with oxygen that terminates the free radicals produced by decomposition of the initiator leading to an inhibition period. Oxygen is consumed in this process and hence its concentration in the liquid phase decreases. A point is reached in which there is not enough oxygen in the liquid phase to terminate all the radicals produced by the initiator and polymerisation starts. However, oxygen does not disappear completely from the liquid phase because more oxygen diffuses from the gas phase. According to this mechanism the higher the concentration of the initiator the more rapidly the initial oxygen is consumed, and hence the shorter the inhibition time. It is expected that the

Table 10 Inhibition periods observed in the different copolymerizations

Run	$N_p \times 10^{-13}$ (particles per cm^3 of water)	$[\text{Na}_2\text{S}_2\text{O}_8] \times 10^7$ (mol cm^{-3} of water)	Seed	N_2 flow	Inhibition period (min)
1C1	24.0	160	AS1	No	0
1C2	24.0	120	AS1	No	0
1C3	24.0	40	AS1	No	0
1C4	24.0	30	AS1	No	0
1C5	24.0	20	AS1	No	1
1C6	24.0	15	AS1	No	3
1C7	24.0	10	AS1	No	4
1C8	47.9	160	AS1	No	0
1C9	47.9	120	AS1	No	0
1C10	47.9	80	AS1	No	0
1C11	47.9	40	AS1	No	0
1C12	47.9	20	AS1	No	1
1C13	47.9	15	AS1	No	2
1C14	47.9	10	AS1	No	3
2C1	10.7	40	AS2	Yes	0
2C2	10.7	20	AS2	Yes	0
2C3	10.7	10	AS2	Yes	3
2C4	10.7	5	AS2	Yes	1
2C5	10.7	2.5	AS2	Yes	14
2C6	10.7	0.625	AS2	Yes	21

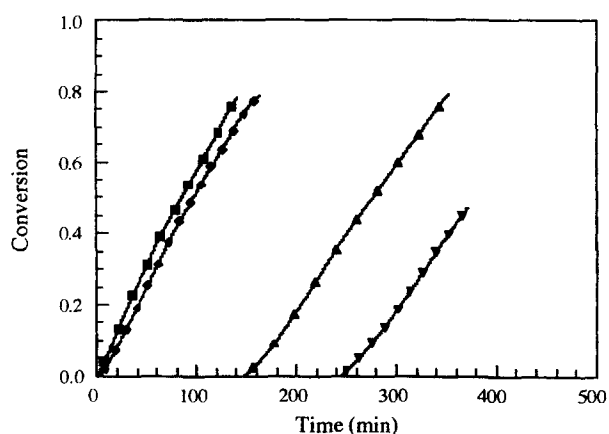


Figure 12 Effect of the nitrogen flow rate on the time evolution of the styrene emulsion homopolymerisation conversion. Legend: (∇) run 3H1 ($0.7 \times 10^{-2} \text{ cm}^3 \text{ s}^{-1}$); (\blacktriangle) run 3H2 ($1.4 \times 10^{-2} \text{ cm}^3 \text{ s}^{-1}$); (\blacklozenge) run 3H3 ($3.0 \times 10^{-2} \text{ cm}^3 \text{ s}^{-1}$); (\blacksquare) run 3H4 ($5.8 \times 10^{-2} \text{ cm}^3 \text{ s}^{-1}$) (seed S1, $N_p = 14.4 \times 10^{13}$ particles per cm^3 of water, $[\text{I}_2] = 2.5 \times 10^{-7} \text{ mol cm}^{-3}$ of water)

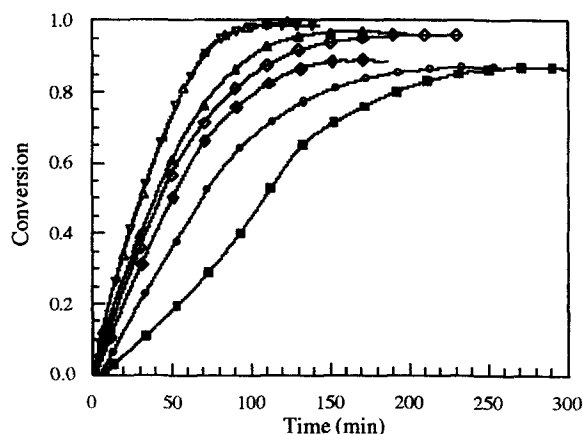


Figure 13 Evolution of the conversion for the first series runs of styrene/butyl acrylate emulsion copolymerisation. (Δ) 1C1, $[\text{I}_2] = 160 \times 10^{-7} \text{ mol cm}^{-3}$ of water; (∇) 1C2, $[\text{I}_2] = 120 \times 10^{-7} \text{ mol cm}^{-3}$ of water; (\blacktriangle) 1C3, $[\text{I}_2] = 40 \times 10^{-7} \text{ mol cm}^{-3}$ of water; (\blacklozenge) 1C4, $[\text{I}_2] = 30 \times 10^{-7} \text{ mol cm}^{-3}$ of water; (\blacklozenge) 1C5, $[\text{I}_2] = 20 \times 10^{-7} \text{ mol cm}^{-3}$ of water; (\circ) 1C6, $[\text{I}_2] = 15 \times 10^{-7} \text{ mol cm}^{-3}$ of water; (\blacksquare) 1C7, $[\text{I}_2] = 10 \times 10^{-7} \text{ mol cm}^{-3}$ of water (seed AS1, $N_p = 24 \times 10^{13}$ particles per cm^3 of water)

inhibition period increases when the total amount of initiator decreases, and this was observed in the reactions 1H2–1H5–1H8 and 1H13–1H17–1H20, in which the total amount of initiator decreased because the volume of the aqueous phase decreased. This mechanism also justifies the effect of the head space/liquid-phase volume ratio because the rate of oxygen mass transfer per volume unit of liquid phase, and hence the extent of its effect, increases with the head space/liquid-phase volume ratio.

In the second series of experiments (Runs 2H1–2H7), both the reaction mixture (without initiator) and the reactor were purged with nitrogen prior the polymerisation, although no flow of nitrogen was used during the polymerisation. The evolution of the conversion in this series of experiments is plotted in *Figures 9 and 10*. The values reported in *Table 8* show that the inhibition periods of this set of experiments are much smaller than the previous ones (without any nitrogen purge). *Figure 11* presents a comparison of the values of \bar{n} calculated at $x = 0.1$ in this series with those calculated in the first series using the same seed and the same particle concentration. It can be seen that higher values of \bar{n} and subsequently higher values of the polymerisation rates were observed in the second series of runs, due to the presence of a smaller amount of oxygen to react with the radicals dissolved in both the water phase and the polymer particles.

The third series of experiments (Runs 3H1–3H4) was carried out using varying flow rates of nitrogen in the preparation of the reaction. In addition, a very low concentration of initiator ($2.5 \times 10^{-7} \text{ mol cm}^{-3}$ of water) was used to enhance the inhibiting effect of the oxygen. *Figure 12* shows that the higher the nitrogen flow rate the higher the polymerisation rate and the lower the inhibition period observed. Some runs using even higher nitrogen flow rates were carried out but an excessive loss of monomer was observed. *Table 8* shows that no inhibition period was observed when a high enough flow rate of nitrogen was used.

Styrene/butyl acrylate emulsion copolymerisation

Figures 13 and 14 present the evolution of the overall conversion of the first series of runs of styrene/butyl acrylate emulsion copolymerisation carried out without elimination

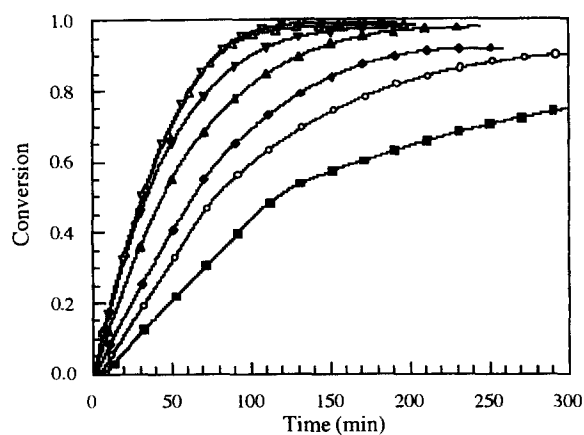


Figure 14 Evolution of the conversion for the first series runs of styrene/butyl acrylate emulsion copolymerisation. (Δ) 1C8, $[I_2] = 160 \times 10^{-7} \text{ mol cm}^{-3}$ of water; (∇) 1C9, $[I_2] = 120 \times 10^{-7} \text{ mol cm}^{-3}$ of water; (\blacktriangledown) 1C10, $[I_2] = 80 \times 10^{-7} \text{ mol cm}^{-3}$ of water; (\blacktriangle) 1C11, $[I_2] = 40 \times 10^{-7} \text{ mol cm}^{-3}$ of water; (\blacklozenge) 1C12, $[I_2] = 20 \times 10^{-7} \text{ mol cm}^{-3}$ of water; (\circ) 1C13, $[I_2] = 15 \times 10^{-7} \text{ mol cm}^{-3}$ of water; (\blacksquare) 1C14, $[I_2] = 10 \times 10^{-7} \text{ mol cm}^{-3}$ of water (seed AS1, $N_p = 47.9 \times 10^{13}$ particles per cm^3 of water)

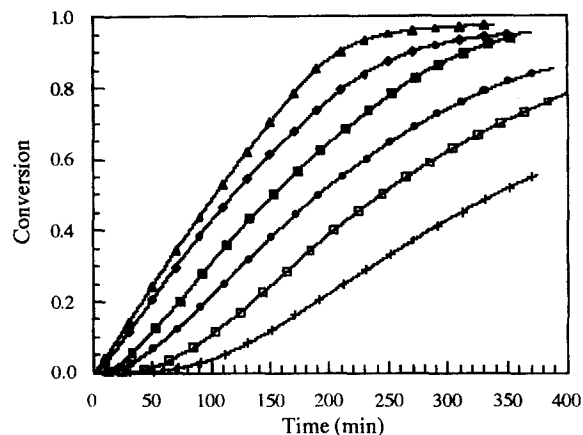


Figure 16 Evolution of the conversion for the second series runs of styrene/butyl acrylate emulsion copolymerisation. (\blacktriangle) 2C1, $[I_2] = 40 \times 10^{-7} \text{ mol cm}^{-3}$ of water; (\blacklozenge) 2C2, $[I_2] = 20 \times 10^{-7} \text{ mol cm}^{-3}$ of water; (\blacksquare) 2C3, $[I_2] = 10 \times 10^{-7} \text{ mol cm}^{-3}$ of water; (\bullet) 2C4, $[I_2] = 5 \times 10^{-7} \text{ mol cm}^{-3}$ of water; (\square) 2C5, $[I_2] = 2.5 \times 10^{-7} \text{ mol cm}^{-3}$ of water; ($+$) 2C6, $[I_2] = 0.625 \times 10^{-7} \text{ mol cm}^{-3}$ of water (seed AS2, $N_p = 10.7 \times 10^{13}$ particles per cm^3 of water)

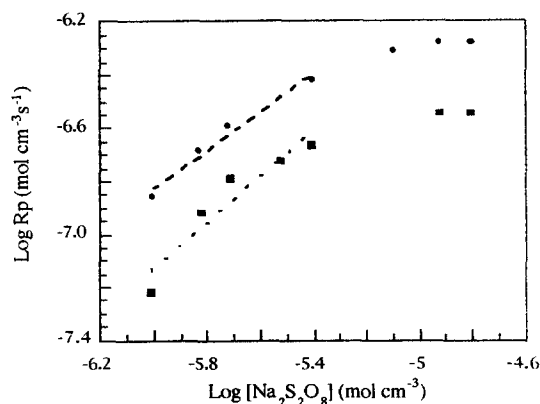


Figure 15 Effect of the initiator concentration on the polymerisation rate measured at $x = 0.1$ for the copolymerisations carried out without nitrogen flow. $N_p \times 10^{-13}$ particles per cm^3 of water: (\blacksquare) 24.0; (\bullet) 47.9

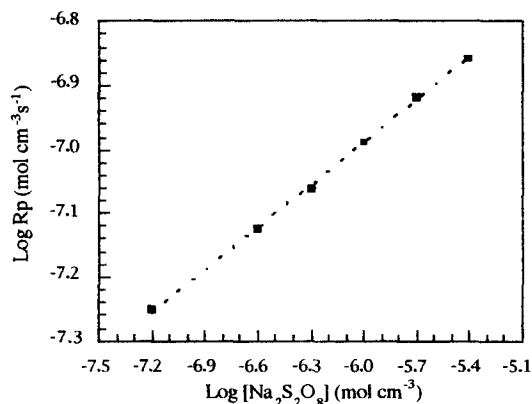


Figure 17 Effect of the initiator concentration on the polymerisation rate measured at $x = 0.15$ for the copolymerisations carried out with a nitrogen purge

Table 11 Values of the \bar{n} ranges and slopes of the runs plotted in *Figures 13 and 14*

Seed	$N_p \times 10^{-13}$ (particles per cm^3 of water)	Slope	Range of \bar{n}
AS1	24.0	0.88	0.09–0.28
AS1	47.9	0.72	0.09–0.25

of oxygen. The inhibition times are summarised in *Table 10*. It can be seen that inhibition is observed only for initiator concentrations smaller than $20 \times 10^{-7} \text{ mol cm}^{-3}$ of water. Furthermore, the inhibition periods are much shorter than the ones observed with styrene. A possible explanation can be related with the smaller head space/liquid-phase volume ratio (half that of the styrene emulsion homopolymerisation runs) which reduces the rate of oxygen mass transfer per volume unit of liquid phase and, hence, decreases the total oxygen amount present in the liquid phase. Moreover, the reactivity towards molecular oxygen of the butyl acryloyl radicals is higher than that of the styryl radicals, due to the delocalising ability of the phenyl ring which promotes a supplementary stabilisation on the styryl radicals with respect to the butyl acryloyl ones. Therefore, the presence of

butyl acrylate will increase the oxygen elimination rate, and will decrease the inhibition period.

Figure 15 shows the dependence of the initiator concentration on the polymerisation rate at 10% overall conversion, for the copolymerisations carried out without nitrogen purge. *Table 11* presents the values of the slopes of the straight lines in *Figure 15*, and the range of average number of radicals per particle calculated taking into account the number of particles and the average $k_p \times [M]_p$ equal to 2000 s^{-1} .²⁶ (Note that the average $k_p \times [M]_p$ can be considered practically constant because the monomer composition in the initial charge is relatively close to the azeotropic composition.) It can be seen that the effect of the initiator concentration is stronger on the reactions carried out with smaller concentration of particles. Furthermore, as was observed in the homopolymerisations, the \bar{n} dependence on the initiator concentration is much higher than that expected theoretically. This point shows again that the oxygen present in the system not only inhibits the reaction but affects the polymerisation rate retarding the polymerisation.

In the series of copolymerisations conducted with nitrogen flow (*Figure 16*), a significant reduction, with respect to the first series of copolymerisations, of the

dependence of R_p on initiator concentration has been observed. The dashed line of *Figure 17* shows a 0.22 power dependence for \bar{n} between 0.17 and 0.40. According to these results, it seems that in this series of experiments, there is no retardation provoked by the oxygen. However, it must be pointed out that, although in this group of polymerisations the dependence of R_p on initiator concentration is smaller, the runs carried out with very small initiator concentrations show inhibition periods (*Table 11*) and a very low evolution of the reaction at the beginning of the process.

CONCLUSIONS

The influence of the oxygen on the kinetics of: (i) the seeded emulsion homopolymerisation of styrene, and (ii) the seeded emulsion copolymerisation of styrene and butyl acrylate, was investigated by reaction calorimetry. Runs with different concentrations of polymer particles, initiator concentration and oxygen levels were carried out. The effect of the head space/liquid-phase volume ratio was also considered.

It was observed that, in seeded emulsion polymerisation systems, the oxygen not only inhibits the reaction, but also retards the reaction rate. Moreover, the dependence of the average number of radicals per particle with the initiator concentration in presence of oxygen was higher than that predicted by theory.

If both the total volume of reaction and the monomer/polymer ratio are held constant, then the inhibition periods due to the presence of oxygen increased when: (a) the initiator concentration decreased, and (b) the concentration of polymer particles increased (for low initiator concentration).

Under conditions of initial oxygen saturation of the reaction mixture, a significant inhibition period was observed for the runs of low initiator concentration. Furthermore, when the ratio between the head space and the liquid phase volume is decreased, an increase of the polymerisation rate and a decrease on the retardation period was observed.

It was also observed that the lower the oxygen level in the reactor, the higher the reaction rate and the lower the inhibition time. Even after the inhibition period, a continuous flow of oxygen from the gas phase is present, which causes the retardation on the polymerisation rate.

ACKNOWLEDGEMENTS

The financial support by the Diputación Foral de Gipuzkoa

and the CICYT (grant MAT 94-0002) are gratefully appreciated. Lourdes López de Arbina and Luis M. Gugliotta acknowledge the fellowships from the Basque Government and the CONICET, respectively.

REFERENCES

1. Odian, G., *Principles of Polymerization*. J. Wiley, NY, 1981.
2. Huo, B. P., Campbell, J. D., Penlidis, A., MacGregor, J. F. and Hamielec, A. E., *J. Appl. Polym. Sci.*, 1988, **35**, 2009.
3. Penlidis, A., MacGregor, J. F. and Hamielec, A. E., *J. Appl. Polym. Sci.*, 1988, **35**, 2023.
4. Penlidis, A., MacGregor, J. F. and Hamielec, A. E., *Polym. Proc. Eng.*, 1985, **3**, 185.
5. Dunn, A. S. and Taylor, P. A., *Makromol. Chem.*, 1965, **83**, 207.
6. Lansdowne, S. W., Gilbert, R. G., Napper, D. H. and Sangster, D. F., *J. Chem. Soc. Faraday I*, 1980, **76**, 1344.
7. Kolthoff, I. M. and Dale, W. J., *J. Am. Chem. Soc.*, 1947, **69**, 441.
8. Ballard, M. J., Napper, D. H. and Gilbert, R. G., *J. Polym. Sci., Polym. Chem. Ed.*, 1984, **22**, 3225.
9. Hasan, S. M., *J. Polym. Sci., Polym. Chem. Ed.*, 1982, **20**, 2969.
10. Schoonbrood, H. A. S., Ph. D. Dissertation, Eindhoven University of Technology, 1994.
11. Adams, M., *Macromolecules*, 1996, **29**, 5751.
12. Vega, J. R., Gugliotta, L. M., Bielsa, R. O., Brandolini, M. C. and Meira, G. R., *Ind. Eng. Chem. Res.*, 1997, **36**, 1238.
13. Hattori, M., Sudol, E. D. and El-Aasser, M. S., *J. Appl. Polym. Sci.*, 1993, **50**, 2027.
14. Burnett, G. M., Lehrle, R. S., Ovenall, D. W. and Peaker, F. W., *J. Polym. Sci.*, 1958, **29**, 417.
15. Kourti, T., Ph. D. Dissertation, McMaster University, 1989.
16. Sáenz, J. M. and Asua, J. M., *J. Polym. Sci. Part A: Polym. Chem.*, 1995, **33**, 511.
17. Nomura, M., Harada, M., Eguchi, W. and Nagata, S., *J. Appl. Polym. Sci.*, 1972, **16**, 835.
18. Kiparissides, C., MacGregor, J. F. and Hamielec, A. E., *AIChE*, 1980, **58**, 48.
19. Donescu, D., Gosa, K. and Languri, J., *Acta Polymerica*, 1990, **41**, 211.
20. Miller, A. A. and Mayo, F. R., *J. Am. Chem. Soc.*, 1956, **78**, 1017.
21. *Kirk-Othmer Encyclopedia of Chemical Technology*. J. Wiley and Sons, 3rd edn., Vol. 16, 1979, p. 654.
22. Buback, M., Gilbert, R. G., Hutchinson, R. A., Klumperman, B., Kuchta, F. D., Manders, B. G., O'Driscoll, K. F., Russell, G. T. and Schweer, J., *Macromol. Chem. Phys.*, 1995, **196**, 3267.
23. Gardon, J. L., *J. Polym. Sci., Part A-1*, 1968, **6**, 643.
24. Ugelstad, J. and Hansen, F. K., *Rubber Chem. Technol.*, 1976, **49**(3), 536.
25. Mørk, P. C., *Eur. Polym. J.*, 1969, **5**, 261.
26. López de Arbina, L., Barandiaran, M. J., Gugliotta, L. M. and Asua, J. M., *Polymer*, 1997, **38**, 143.